On the linear stability of turbulent plane strain flow in a rotating frame

E. Akylas,[a] C. A. Langer, S. C. Kassinos,[b] and E. Demosthenous
Department of Mechanical and Manufacturing Engineering, 75 Kallipoleos, University of Cyprus, Nicosia 1678, Cyprus

(Received 23 February 2007; accepted 24 May 2007; published online 25 July 2007)

We apply inviscid rapid distortion theory to the limiting hyperbolic case of turbulent plain strain flow in a rotating frame and investigate the dependence of the evolution of the turbulent kinetic energy on the frame rotation rate. We derive an analytical two-dimensional solution that, unlike previous oversimplified pressureless analyses, allows for an accurate approximation of the three-dimensional initially isotropic problem. From the analytical solutions, we determine the correct stability criterion for the evolution of the turbulent kinetic energy in this flow. Also, we calculate the asymptotic states of the turbulence, in terms of the normalized Reynolds stresses and structure dimensionality tensor components, which coincide with the exact three-dimensional numerical results. © *2007 American Institute of Physics*. [DOI: 10.1063/1.2750683]

I. INTRODUCTION

The effects of system rotation on quadratic flows have received considerable attention during the past decade because of their relevance to important technological and geophysical problems. Quadratic flows are a special class of two-dimensional flows with uniform mean velocity gradients on a reference frame. They are constituted by different combinations of mean strain and mean flow rotation. Depending on their relative magnitude we may have hyperbolic flows, when rotation is smaller than strain, or elliptic flows, when rotation exceeds strain. The separating case, when they equal each other, is the well known shear case (parallel streamlines).

The presence of rotation of the reference frame can act to either stabilize or destabilize the turbulence, depending on the ratio of the frame rotation rate to that of the mean deformation rate. Numerical studies (see, for example, Refs. 1 and 2) have clearly shown the dependence of the evolution of the turbulent kinetic energy (TKE) on that ratio. However, important details, such as long-time asymptotic states, and the transition limits from the stable to the unstable regimes for a general quadratic flow remain unclear.

Apart from numerical experiments, considerable insight into the evolution of the TKE can be gained through rapid distortion theory (RDT). In the framework of RDT, linearized equations of motion are used to explain some of the significant kinematical and dynamical responses of turbulence to imposed deformation. The theory is valid for rapidly changing turbulent flows, when the distortion is applied for a time that is short compared to the "turnover" time scale of the energy-containing eddies; that is the initial response to a sudden change in the mean deformation. Furthermore, RDT is also a good approximation, in cases in which the ratio of the mean deformation time scale over the eddy "turnover" time scale is much smaller than 1,[3,4] which ensures that the nonlinear terms in the governing turbulence equations involving products of fluctuation quantities are still negligible; then the turbulence is affected mostly by the mean flow and not by the turbulence itself. Thus, under RDT the nonlinear effects resulting from turbulence-turbulence interactions are neglected in the governing equations.[5–7] Simple cases of rapid deformation often admit closed-form solutions for individual Fourier coefficients. The solutions to the linearized equations can be used to calculate the characteristics of the development of the energy spectrum tensor, two-point correlations, and other turbulence statistic quantities of interest.

While shear flows in rotating frames have been a popular case study of both numerical and analytical works, the generalized quadratic flow has not received as much attention. A nice work by Salhi *et al.*[8] investigated the effect of the frame rotation on the stability of the turbulence in the general case, and they introduced a modified Bradshaw[9] number in order to characterize the stability limits. The specific criterion has been derived based on a pressureless analysis,[10] where the pressure fluctuations were omitted from the governing equations. The authors concluded that the modified criterion applies well if the total rotation vanishes, that is, when the reference frame counter-rotates at a rate that cancels the mean flow rotation. A simple case in which this is not applicable, as will be shown here, is the plane strain case (Fig. 1). This is the limiting hyperbolic case, when there is no mean flow rotation (this can also be understood as the limit of a very large ratio of mean strain to mean rotation).

In order to contribute to the understanding of this case, in the present study we use RDT to investigate the evolution of the turbulence in plane strain flow, subject to frame rotation. This study refers especially to the stability limits for the evolution of the TKE and extends to the development of the Reynolds stresses $R_{ij}=\overline{u_i u_j}$ and the structure dimensionality tensor D_{ij}.[11] The combined use of these tensors allows one to distinguish between the componentality of the turbulence (described by R_{ij}) and its dimensionality, which has to do

[a]Also with the Institute of Environmental Research, National Observatory of Athens, Greece.
[b]Author to whom correspondence should be addressed. Also with the Center for Turbulence Research, Stanford University/NASA-Ames. Electronic mail: kassinos@ucy.ac.cy

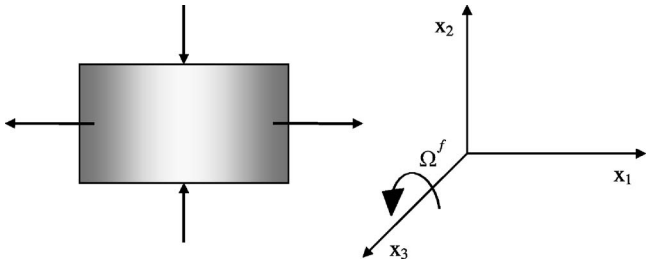

FIG. 1. Schematic illustration of the plane strain flow in a rotating frame that is examined here.

with the morphology of the turbulence eddies, and is described by D_{ij}. For example, if $D_{11}=0$, then the turbulence is independent of the x_1 axis, that is, it consists of long structures aligned with the x_1 direction.

Apart from the general interest in understanding the effect of plane strain on turbulent flows, a strong motivation for this study arose from our efforts to develop an algebraic structure-based turbulence model, which has been successfully used, so far, to compute the characteristics of rotating turbulent channel and boundary layer flow.[12] The model uses RDT asymptotic limits as targets or guidelines for determining the anisotropy of the Reynolds stress and structure dimensionality tensors under strong deformations, aiming to improve model dependability and reliability. While the RDT asymptotics for the shear case are known (see, for example, Akylas *et al.*[13]), the respective information for the plane strain case is introduced in this study.

The present paper is organized as follows. In Sec. II, we present the basic linearized RDT equations for the general three-dimensional (3D) and three-componental (3C) case of plane strain in a rotating frame. In Sec. III, we investigate a pressureless solution and we show its inability to describe accurately the stability limits of the initially 3D-3C isotropic case. In Sec. IV, we solve analytically an alternative 2D-3C case (referring to the approximated 2D character of the turbulent eddies), which maintains the pressure effects, and in Sec. V we calculate asymptotic expressions for the stresses and the TKE evolution. The 2D (but 3C) results regarding the TKE, the stresses, and the structure dimensionality tensor components are compared, in Sec. VI, against the 3D numerical solution obtained with the particle representation model (PRM), which has been developed by Kassinos and Reynolds,[14] and they show remarkable agreement.

II. LINEAR EQUATIONS

In the case of plane strain with frame rotation (Fig. 1), the mean strain rate, mean rotation rate (zero), and frame rotation rate tensors are

$$S_{ij}^{*}=\begin{pmatrix}\Gamma & 0 & 0\\ 0 & -\Gamma & 0\\ 0 & 0 & 0\end{pmatrix},\quad \Omega_{ij}=\begin{pmatrix}0 & 0 & 0\\ 0 & 0 & 0\\ 0 & 0 & 0\end{pmatrix},$$
$$\Omega_{ij}^{f}=\begin{pmatrix}0 & -\Omega^{f} & 0\\ \Omega^{f} & 0 & 0\\ 0 & 0 & 0\end{pmatrix}. \tag{2.1}$$

For the general three-dimensional and three-componental (3D-3C) case, the inviscid linear RDT equations for the fluctuating velocity components become

$$\frac{\partial u_i}{\partial t}+\Gamma x_1\frac{\partial u_i}{\partial x_1}-\Gamma x_2\frac{\partial u_i}{\partial x_2}=-\Gamma u_i(\delta_{i1}-\delta_{i2})-\frac{1}{\rho}\frac{\partial p}{\partial x_i}+2\varepsilon_{ij3}\Omega^f u_j. \tag{2.2}$$

Using the Rogallo[15] transformation, we set

$$\xi_1=x_1e^{-\Gamma t},\quad \xi_2=x_2e^{\Gamma t},\quad \xi_3=x_3,\quad \tau=t, \tag{2.3}$$

and (2.2) transforms to

$$\frac{\partial u_1}{\partial \tau}=-\Gamma u_1-\frac{1}{\rho}\frac{\partial p}{\partial \xi_1}e^{-\Gamma t}+2\Omega^f u_2,$$
$$\frac{\partial u_2}{\partial \tau}=\Gamma u_2-\frac{1}{\rho}\frac{\partial p}{\partial \xi_2}e^{\Gamma t}-2\Omega^f u_1, \tag{2.4}$$
$$\frac{\partial u_3}{\partial \tau}=-\frac{1}{\rho}\frac{\partial p}{\partial \xi_3}.$$

Applying the Fourier transformation to (2.4), the coefficients (denoted with ^) in the spectral space evolve as

$$\frac{\partial \hat{u}_1}{\partial \tau}=-\Gamma \hat{u}_1+\frac{i\hat{p}}{\rho}k_1e^{-\Gamma t}+2\Omega^f\hat{u}_2,$$
$$\frac{\partial \hat{u}_2}{\partial \tau}=\Gamma \hat{u}_2+\frac{i\hat{p}}{\rho}k_2e^{\Gamma t}-2\Omega^f\hat{u}_1, \tag{2.5}$$
$$\frac{\partial \hat{u}_3}{\partial \tau}=\frac{i\hat{p}}{\rho}k_3.$$

Substituting the Fourier transformed continuity equation, $k_1e^{-\beta}\hat{u}_1+k_2e^{\beta}\hat{u}_2+k_3\hat{u}_3=0$, we can solve for the pressure in (2.5),

$$\frac{i\hat{p}}{\rho}=\frac{2\Gamma k_1e^{-\Gamma t}\hat{u}_1-2\Gamma k_2e^{\Gamma t}\hat{u}_2-k_1e^{-\Gamma t}2\Omega^f\hat{u}_2+k_2e^{\Gamma t}2\Omega^f\hat{u}_1}{(k_1^2e^{-2\Gamma t}+k_2^2e^{2\Gamma t}+k_3^2)}, \tag{2.6}$$

and by substituting (2.6) into the system (2.5), this simplifies to

$$\frac{\partial \hat{u}_1}{\partial \beta} = \frac{(k_1^2 e^{-2\beta} - k_2^2 e^{2\beta} - k_3^2 + \eta k_1 k_2)\hat{u}_1 + (\eta k_2^2 e^{2\beta} + \eta k_3^2 - 2k_1 k_2)\hat{u}_2}{(k_1^2 e^{-2\beta} + k_2^2 e^{2\beta} + k_3^2)},$$

$$\frac{\partial \hat{u}_2}{\partial \beta} = \frac{(k_1^2 e^{-2\beta} - k_2^2 e^{2\beta} + k_3^2 - k_1 k_2 \eta)\hat{u}_2 - (\eta k_1^2 e^{-2\beta} + \eta k_3^2 - 2k_1 k_2)\hat{u}_1}{(k_1^2 e^{-2\beta} + k_2^2 e^{2\beta} + k_3^2)}, \tag{2.7}$$

$$\frac{\partial \hat{u}_3}{\partial \beta} = k_3 \frac{2k_1 e^{-\beta}\hat{u}_1 - 2k_2 e^{\beta}\hat{u}_2 - k_1 e^{-\beta}\eta\hat{u}_2 + k_2 e^{\beta}\eta\hat{u}_1}{(k_1^2 e^{-2\beta} + k_2^2 e^{2\beta} + k_3^2)},$$

where $\beta = \Gamma\tau$ is the total strain applied, and $\eta = 2\Omega^f/\Gamma$ is the dimensionless frame rotation rate. Solutions of this system in terms of the spectrum components $E_{ij} \sim \overline{\hat{u}_i \hat{u}_j^*}$ for the specific case without frame rotation ($\eta = 0$) have been reported by Lagnado *et al.*[16] and Lee *et al.*[17] Such solutions were used for the approximation of the Reynolds stresses, $R_{ij} = \overline{u_i u_j} = \iiint_{\mathbf{k}} E_{ij} d^3\mathbf{k}$ at large total strain, which in this case reach the following unstable asymptotic behavior (this has also been reported much earlier by Townsend[5] in his equations 3.11.10):

$$R_{11}/q_0^2 \sim \beta e^{-\beta}, \quad R_{22}/q_0^2 \sim e^{\beta}, \quad R_{33}/q_0^2 \sim e^{\beta}, \tag{2.8}$$

where q_0^2 is twice the initial kinetic energy. However, a general analytical solution of the 3D system in the case of frame rotation is not known as of yet. Fortunately, we may draw some of the main characteristics of the 3D solution by carrying out simplified 1D or 2D analyses, as will be shown. More specifically, the 3D system (2.7) can be simplified by setting specific components of the wave-number vector equal to 0. In such cases, it is possible to derive analytical solutions for the evolution of the spectra of the turbulence, as shown in Secs. III and IV. By integrating the spectra over all the wave numbers, we obtain solutions in physical space, for the development of the stress components and the structure dimensionality tensor (see Refs. 11 and 13),

$$D_{ij} = \int \int \int_{\mathbf{k}} E_{nn}(\mathbf{k}) \frac{k_i k_j}{k^2} d^3\mathbf{k} \tag{2.9}$$

and its normalized form

$$d_{ij} = D_{ij}/D_{kk} = D_{ij}/R_{kk} = D_{ij}/q^2, \quad \text{where } q^2 = R_{ii} = 2 \times \text{TKE}. \tag{2.10}$$

III. PRESSURELESS ANALYSIS ($k_3 \neq 0$)

As mentioned, the 3D system (2.7) can be simplified using 1D or 2D initializations (setting specific wave numbers to 0) making it amenable to analytical solutions. For instance, setting $k_1 = 0$ means that the turbulence is initially composed of eddies that are elongated in the direction of the mean flow (x_1 axis). For the simpler 1D cases, we may alternatively use three different 1D (for example $k_2 = k_3 = 0$) initializations. A simple pressureless approach is quite often used[2,8] in order to help to identify some of the main characteristics regarding the behavior of the RDT equations. Neglecting the pressure terms from the RDT equations (2.2) is equivalent, for the specific case at hand, to a 1D-2C analysis of the problem, with $k_1 = k_2 = 0$, $k_3 \neq 0$. This can be easily understood since, in the 1D case, where there is only dependence on the x_3 direction, Eqs. (2.2) simplify to

$$\partial u_1/\partial\beta = -u_1 + \eta u_2, \quad \partial u_2/\partial\beta = u_2 - \eta u_1, \quad \partial u_3/\partial\beta = 0. \tag{3.1}$$

The same equation for the Fourier transformed velocity components can also be obtained by simply setting $k_1 = k_2 = 0$ in (2.7). In the above pressureless formulation, the solution for the evolution of the velocity components yields

$$u_1 = u_1^0 \cosh(\beta\sqrt{1-\eta^2}) + (\eta u_2^0 - u_1^0)\sinh(\beta\sqrt{1-\eta^2})/\sqrt{1-\eta^2},$$

$$u_2 = u_2^0 \cosh(\beta\sqrt{1-\eta^2}) - (\eta u_1^0 - u_2^0)\sinh(\beta\sqrt{1-\eta^2})/\sqrt{1-\eta^2}, \tag{3.2}$$

$$u_3 = 0,$$

which depends on the dimensionless rotation of the frame, resulting in an exponential growth of the TKE with time, for $\eta^2 < 1$. For values of η^2 larger than 1, the stresses oscillate and the TKE stabilizes, around a constant value. The same limit for the stabilization of the TKE in the case of plane strain with frame rotation has been reported by Salhi *et al.*[8] based on their pressureless analysis of a generalized quadratic flow. More specifically, their modified Bradshaw number, Br, which characterizes the stability of the TKE, reduces for the plane strain flow to $\text{Br} = 1 - \eta^2$ (see also Godeferd[18]). However, the above limit for the stabilization of the TKE does not match the one shown in Fig. 3 in the exact solution (using the PRM representation) of the initially homogeneous 3D case. The 3D numerical solution reveals that the TKE approaches a stable behavior for values of η between 0.85 and 0.90. This implies that the role of the pressure fluctuations is crucial for the evolution of the turbulence, especially through the rapidly evolving wave-vector component $k_2 e^{\beta}$ in (2.6) and (2.7). This inability of the pressureless formulation to identify the stability limits in general quadratic flows correctly, compared to the "true" linear analysis (where the pressure terms are present), has been pointed out by Salhi.[8] In the following, we examine the plane strain flow using a 2D approach, which maintains the pressure fluctuations, resulting

in an accurate characterization of the stability dependence on the rotation of the frame.

IV. TWO-DIMENSIONAL ANALYTICAL SOLUTION FOR $k_1=0$

By setting only $k_1=0$, we introduce a more appropriate 2D (but 3C) case, where the turbulence is independent of the x_1 direction. We could also set $k_2=0$ or $k_3=0$, instead of $k_1=0$, forcing the turbulence to be independent of the x_2 or x_3 directions, respectively. However, we have found that the choice $k_1=0$ yields a subsequent evolution of the turbulence statistics that is much closer to the one obtained using the 3D isotropic initialization. This can be explained by the fact that in the 3D equations (2.7), the dependence on x_1 vanishes rapidly, since the wave-number component k_1 is multiplied by $e^{-\beta}$. Thus, the general 3D case evolves fast toward a 2D behavior with a vanishing normalized dimensionality component $d_{11}=D_{11}/q^2\to 0$, as illustrated in Fig. 4 for several values of η. For the specific choice of $k_1=0$, the 3D system (2.7) simplifies to

$$\frac{\partial \hat{u}_1}{\partial \beta}=-\hat{u}_1+\eta\hat{u}_2,$$

$$\frac{\partial \hat{u}_2}{\partial \beta}=\frac{k_3^2\hat{u}_2-k_2^2e^{2\beta}\hat{u}_2-k_3^2\eta\hat{u}_1}{k_2^2e^{2\beta}+k_3^2}, \tag{4.1}$$

$$\frac{\partial \hat{u}_3}{\partial \beta}=\frac{-2k_3k_2e^{\beta}\hat{u}_2+k_3k_2e^{\beta}\eta\hat{u}_1}{k_2^2e^{2\beta}+k_3^2}.$$

The solution of (4.1) is a complicated task, especially regarding the subsequent integrations for the calculation of the one-point structure tensors, as it is not possible to derive fully analytical expressions. However, we may draw important conclusions based on the investigation of the behavior of the spectral solution. Equation (4.1) can be written in the form

$$\frac{\partial \hat{u}_1}{\partial \beta}=-\hat{u}_1+\eta\hat{u}_2,$$

$$(1+\theta^2e^{2\beta})\frac{\partial \hat{u}_2}{\partial \beta}=(1-\theta^2e^{2\beta})\hat{u}_2-\eta\hat{u}_1, \tag{4.2}$$

$$(\theta^2e^{2\beta}+1)\frac{\partial \hat{u}_3}{\partial \beta}=\theta e^{\beta}(-2\hat{u}_2+\eta\hat{u}_1),$$

where θ depends on the initial wave-number components as $\theta^2=k_2^2/k_3^2$, which, in polar coordinates (setting $k_2=k_0\cos\varphi$ and $k_3=k_0\sin\varphi$, with $k_0^2=k_2^2+k_3^2$) corresponds to $\theta^2=\cot^2\varphi$. After some algebra, (4.2) yields

$$(1+e^{2\beta}\theta^2)\frac{\partial^2\hat{u}_1}{\partial\beta^2}+2e^{2\beta}\theta^2\frac{\partial\hat{u}_1}{\partial\beta}+(\eta^2-1+e^{2\beta}\theta^2)\hat{u}_1=0,$$

$$(1+\theta^2e^{2\beta})\frac{\partial^2\hat{u}_2}{\partial\beta^2}+4\theta^2e^{2\beta}\frac{\partial\hat{u}_2}{\partial\beta}+(\eta^2-1+3\theta^2e^{2\beta})\hat{u}_2=0, \tag{4.3}$$

$$\hat{u}_3=-\theta e^{\beta}\hat{u}_2.$$

Setting $z=\theta^2e^{2\beta}$ and $\hat{v}_i=\hat{u}_ie^{\beta}$, the system (4.3) transforms to

$$z^2(1+z)\frac{\partial^2\hat{v}_1}{\partial z^2}+z^2\frac{\partial\hat{v}_1}{\partial z}+\frac{\eta^2}{4}\hat{v}_1=0,$$

$$z^2(1+z)\frac{\partial^2\hat{v}_2}{\partial z^2}+2z^2\frac{\partial\hat{v}_2}{\partial z}+\frac{\eta^2}{4}\hat{v}_2=0. \tag{4.4}$$

The general solution of (4.4) is derived in the following form:

$$\hat{v}_1(z)=C_1z^{a_+}F(a_+,a_+;2a_+;-z)+C_2z^{a_-}F(a_-,a_-;2a_-;-z),$$

$$\hat{v}_2(z)=C_3z^{a_+}F(a_+,1+a_+;2a_+;-z)+C_4z^{a_-}F(a_-,1+a_-;2a_-;-z), \tag{4.5}$$

where C_1–C_4 are parameters, which have to be calculated by the initial conditions, and $F(a,b;c;z)$ is the hypergeometric function, with the parameters $a_\pm$ depending on η as

$$a_\pm=\frac{(1\pm\sqrt{1-\eta^2})}{2}. \tag{4.6}$$

Using the transformation formula

$$F(a,b;c;z)=(1-z)^{-a}F\left(a,c-b;c;\frac{z}{z-1}\right) \tag{4.7}$$

allows a useful argument change resulting in

$$\hat{v}_1(z)=C_1z^{a_+}(1+z)^{-a_+}F\left(a_+,a_+;2a_+;\frac{z}{1+z}\right)+C_2z^{a_-}(1+z)^{-a_-}F\left(a_-,a_-;2a_-;\frac{z}{1+z}\right),$$

$$\hat{v}_2(z)=C_3z^{a_+}(1+z)^{-a_+}F\left(a_+,-a_-;2a_+;\frac{z}{1+z}\right)+C_4z^{a_-}(1+z)^{-a_-}F\left(a_-,-a_+;2a_-;\frac{z}{1+z}\right). \tag{4.8}$$

Writing (4.8) in terms of the original velocity Fourier components $\hat{u}_i(\beta,\varphi,\eta)=\hat{v}_i(z,\eta)e^{-\beta}$, and using the initial conditions

$$\left.\frac{\partial \hat{u}_1}{\partial \beta}\right|_{\beta=0} = -\hat{u}_1^0 + \eta \hat{u}_2^0,$$
$$\left.\frac{\partial \hat{u}_2}{\partial \beta}\right|_{\beta=0} = \frac{(1-\theta^2)\hat{u}_2^0 - \eta \hat{u}_1^0}{(1+\theta^2)} \tag{4.9}$$

(where the superscript 0 denotes initial values), the spectral solution is derived,

$$\hat{u}_1 = \frac{e^{\beta\sqrt{1-\eta^2}}[(A_1^+\hat{u}_1^0 + A_2^+\hat{u}_2^0) - e^{-2\beta\sqrt{1-\eta^2}}(A_1^-\hat{u}_1^0 + A_2^-\hat{u}_2^0)]}{A(\sin^2\varphi + e^{2\beta}\cos^2\varphi)^{1/2}},$$

$$\hat{u}_2 = \frac{e^{\beta\sqrt{1-\eta^2}}[(B_1^+\hat{u}_1^0 + B_2^+\hat{u}_2^0) - e^{-2\beta\sqrt{1-\eta^2}}(B_1^-\hat{u}_1^0 + B_2^-\hat{u}_2^0)]}{B(\sin^2\varphi + e^{2\beta}\cos^2\varphi)^{1/2}}, \tag{4.10}$$

$$\hat{u}_3 = -e^{\beta}\cot\varphi\,\hat{u}_2.$$

The coefficients A, B, $A_i^{\pm}$, and $B_i^{\pm}$ are given in terms of hypergeometric functions,

$$\begin{aligned} A_1^{\pm} &= a_{\mp}(\sin^2\varphi + e^{2\beta}\cos^2\varphi)^{\mp\sqrt{1-\eta^2}/2} \\ &\quad\times F\left(a_{\pm},a_{\pm};2a_{\pm};\frac{\cos^2\varphi}{\cos^2\varphi + e^{-2\beta}\sin^2\varphi}\right) \\ &\quad\times[2F(a_{\mp},a_{\mp};2a_{\mp};\cos^2\varphi) - \cos^2\varphi \\ &\quad\times F(1+a_{\mp},a_{\mp};1+2a_{\mp};\cos^2\varphi)], \end{aligned}$$

$$\begin{aligned} A_2^{\pm} &= \eta(\sin^2\varphi + e^{2\beta}\cos^2\varphi)^{\mp\sqrt{1-\eta^2}/2} \\ &\quad\times F(a_{\mp},a_{\mp};2a_{\mp};\cos^2\varphi) \\ &\quad\times F\left(a_{\pm},a_{\pm};2a_{\pm};\frac{\cos^2\varphi}{\cos^2\varphi + e^{-2\beta}\sin^2\varphi}\right), \end{aligned}$$

$$\begin{aligned} A &= a_-\cos^2\varphi F(1+a_-,a_-;1+2a_-;\cos^2\varphi) \\ &\quad\times F(a_+,a_+;2a_+;\cos^2\varphi) + F(a_-,a_-;2a_-;\cos^2\varphi) \\ &\quad\times [2\sqrt{1-\eta^2}F(a_+,a_+;2a_+;\cos^2\varphi) \\ &\quad - a_+\cos^2\varphi F(1+a_+,a_+;1+2a_+;\cos^2\varphi)], \end{aligned} \tag{4.11}$$

$$\begin{aligned} B_1^{\pm} &= \eta(\sin^2\varphi + e^{2\beta}\cos^2\varphi)^{\mp\sqrt{1-\eta^2}/2}\sin^2\varphi \\ &\quad\times F(a_{\mp},-a_{\pm};2a_{\mp};\cos^2\varphi) \\ &\quad\times F\left(a_{\pm},-a_{\mp};2a_{\pm};\frac{\cos^2\varphi}{\cos^2\varphi + e^{-2\beta}\sin^2\varphi}\right), \end{aligned}$$

$$\begin{aligned} B_2^{\pm} &= (\sin^2\varphi + e^{2\beta}\cos^2\varphi)^{\mp\sqrt{1-\eta^2}/2} \\ &\quad\times F\left(a_{\pm},-a_{\mp};2a_{\pm};\frac{\cos^2\varphi}{\cos^2\varphi + e^{-2\beta}\sin^2\varphi}\right) \\ &\quad\times[2(a_{\pm}\sin^2\varphi - a_{\mp}\cos^2\varphi)F(a_{\mp},-a_{\pm};2a_{\mp};\cos^2\varphi) \\ &\quad + (1+a_{\mp})\cos^2\varphi F(1+a_{\mp},-a_{\pm};1+2a_{\mp};\cos^2\varphi)], \end{aligned}$$

$$\begin{aligned} B &= (1+a_-)\cos^2\varphi F(1+a_-,-a_+;1+2a_-;\cos^2\varphi) \\ &\quad\times F(a_+,-a_-;2a_+;\cos^2\varphi) + F(a_-,-a_+;2a_-;\cos^2\varphi) \\ &\quad\times [2\sqrt{1-\eta^2}F(a_+,-a_-;2a_+;\cos^2\varphi) \\ &\quad - (1+a_+)\cos^2\varphi F(1+a_+,-a_-;1+2a_+;\cos^2\varphi)]. \end{aligned}$$

The limit of the above solutions (4.10) and (4.11) when $\varphi = \pi/2$ is identical to the pressureless analysis limit, where the equations reduce to (3.2). However, the contribution of the whole range of φ must be taken into account. More specifically, as φ departs from $\pi/2$ toward $\boldsymbol{\varphi}=0$ or $\boldsymbol{\varphi}=\pi$, the Fourier coefficients decrease symmetrically. At exactly $\boldsymbol{\varphi}=0$ or $\boldsymbol{\varphi}=\pi$, the solution becomes independent of η, in agreement with the principle of *material indifference*[19] for 2D turbulence independent of the axis of the frame rotation ($k_3=0$),

$$\hat{u}_1(\varphi=0) = \hat{u}_1^0 e^{-\beta}, \quad \hat{u}_2(\varphi=0) = 0, \quad \hat{u}_3(\varphi=0) = \hat{u}_3^0. \tag{4.12}$$

This shows that the Fourier modes approach constant values; the fluctuations do not grow with time. The contribution of the full range of φ, $0 \le \varphi \le \pi$, results in remarkable modifications regarding the TKE evolution. This is shown in the next section, where we derive the velocity spectrum tensor components, $E_{ij} \sim \overline{\hat{u}_i \hat{u}_j^*}$, and their corresponding Reynolds stresses.

V. EVOLUTION OF THE STRESSES AND THE TKE

In order to calculate and integrate the spectra for the derivation of the Reynolds stresses and, consequently, the TKE, we make use of two different initializations, namely a *vortical* and a *jetal* initial velocity spectrum.[11–13] More specifically, in the vortical case the componentality of the initially strictly 2D turbulence is isotropic in planes perpendicular to the axis of independence (x_1 in our case). In this case, the vortical 2D-2C spectrum is given by (see also Cambon *et al.*[20])

$$E_{ij}^{\text{vor}}(k,0) = \frac{E(k,0)}{2\pi k}\delta(k_1)\left(\delta_{ij} - \frac{k_i k_j}{k^2} - \delta_{i1}\delta_{j1}\right),$$
$$i = 1,2,3 \quad j = 1,2,3. \tag{5.1}$$

In contrast, when the initial turbulence is completely jetal, all the velocity fluctuations are in the direction of the axis of independence x_1. The initial 2D-1C jetal spectrum corresponding to this condition is

$$E_{ij}^{\text{jet}}(k,0) = \frac{E(k,0)}{2\pi k}\delta(k_1)\delta_{i1}\delta_{j1} \quad \text{for } i = 1,2,3 \quad j = 1,2,3. \tag{5.2}$$

In the relations (5.1) and (5.2), the initial turbulent kinetic energy spectrum $E(k,0)$ satisfies

$$\int_{k=0}^{\infty} E(k,0)dk = R_{ii}^0/2 = q_0^2/2. \tag{5.3}$$

Because of the linearity of the governing equations, the energy spectra for the initially jetal 2D-1C and the vortical 2D-2C cases can be superposed to produce (after integration over the wave numbers) R_{ij} and D_{ij} for various 2D-3C initial fields, consisting of uncorrelated jets and vortices.[11–13] As pointed out by an anonymous referee, such a superposition yields the so-called two-dimensional energy components,[5,20] i.e., the product of the Reynolds stress tensor, by associated integral length scales in the x_1 direction, $L_{ij}^{(1)}$, or equivalently, the limit of the spectra at $k_1=0$, $\varepsilon_{ij}^{(1)}(\beta)=\pi\int\int E_{ij}(k_1=0,k_2,k_3,\beta)e^{\beta}dk_2dk_3$.

When an initially vortical velocity spectrum (5.1) is used, the solution (4.6) for the Fourier transformed velocity components results in the evolution of the spectrum components,

$$E_{11}^{\text{vor}} = e^{-2\beta\sqrt{1-\eta^2}}(\sin^2\varphi + e^{2\beta}\cos^2\varphi)^{-1}\left(e^{2\beta\sqrt{1-\eta^2}}\frac{A_2^+}{A} - \frac{A_2^-}{A}\right)$$
$$\times\left(e^{2\beta\sqrt{1-\eta^2}}\frac{A_2^+}{A} - \frac{A_2^-}{A}\right)^* E_{22}^0,$$

$$E_{22}^{\text{vor}} = e^{-2\beta\sqrt{1-\eta^2}}(\sin^2\varphi + e^{2\beta}\cos^2\varphi)^{-1}\left(e^{2\beta\sqrt{1-\eta^2}}\frac{B_2^+}{B} - \frac{B_2^-}{B}\right)$$
$$\times\left(e^{2\beta\sqrt{1-\eta^2}}\frac{B_2^+}{B} - \frac{B_2^-}{B}\right)^* E_{22}^0, \tag{5.4}$$

$$E_{12}^{\text{vor}} = \frac{A_2^+B_2^{+*}e^{4\beta\sqrt{1-\eta^2}} - (A_2^+B_2^{-*} + A_2^-B_2^{+*})e^{2\beta\sqrt{1-\eta^2}} + A_2^-B_2^{-*}}{AB^*(\sin^2\varphi + e^{2\beta}\cos^2\varphi)e^{2\beta\sqrt{1-\eta^2}}}E_{22}^0,$$

where * denotes a complex conjugate. In the case of a jetal initialization (5.2), the respective spectral solution takes the form

$$E_{11}^{\text{jet}} = e^{-2\beta\sqrt{1-\eta^2}}(\sin^2\varphi + e^{2\beta}\cos^2\varphi)^{-1}\left(e^{2\beta\sqrt{1-\eta^2}}\frac{A_1^+}{A} - \frac{A_1^-}{A}\right)$$
$$\times\left(e^{2\beta\sqrt{1-\eta^2}}\frac{A_1^+}{A} - \frac{A_1^-}{A}\right)^* E_{11}^0,$$

$$E_{22}^{\text{jet}} = e^{-2\beta\sqrt{1-\eta^2}}(\sin^2\varphi + e^{2\beta}\cos^2\varphi)^{-1}\left(e^{2\beta\sqrt{1-\eta^2}}\frac{B_1^+}{B} - \frac{B_1^-}{B}\right)$$
$$\times\left(e^{2\beta\sqrt{1-\eta^2}}\frac{B_1^+}{B} - \frac{B_1^-}{B}\right)^* E_{11}^0, \tag{5.5}$$

$$E_{12}^{\text{jet}} = \frac{A_1^+B_1^{+*}e^{4\beta\sqrt{1-\eta^2}} - (A_1^+B_1^{-*} + A_1^-B_1^{+*})e^{2\beta\sqrt{1-\eta^2}} + A_1^-B_1^{-*}}{AB^*(\sin^2\varphi + e^{2\beta}\cos^2\varphi)e^{2\beta\sqrt{1-\eta^2}}}E_{11}^0.$$

For values of $\eta^2 \le 1$, when the parameters $a_\pm$ are real numbers [Eq. (4.5)], the Reynolds stress components R_{11}, R_{22}, and R_{12}, resulting from the integration of the spectral relations over all wave numbers, approach fast the following behavior:

$$R_{ij}^{\text{vor}} \to \frac{q_0^2}{\pi}e^{2\beta\sqrt{1-\eta^2}}\int_0^{\pi}\left(\frac{A_2^+}{A}\delta_{i1} + \frac{B_2^+}{B}\delta_{i2}\right)\left(\frac{A_2^+}{A}\delta_{j1} + \frac{B_2^+}{B}\delta_{j2}\right)^*$$
$$\times\sin^2\varphi(\sin^2\varphi + e^{2\beta}\cos^2\varphi)^{-1}d\varphi,$$
$$R_{ij}^{\text{jet}} \to \frac{q_0^2}{\pi}e^{2\beta\sqrt{1-\eta^2}}\int_0^{\pi}\left(\frac{A_1^+}{A}\delta_{i1} + \frac{B_1^+}{B}\delta_{i2}\right)\left(\frac{A_1^+}{A}\delta_{j1} + \frac{B_1^+}{B}\delta_{j2}\right)^* \tag{5.6}$$
$$\times(\sin^2\varphi + e^{2\beta}\cos^2\varphi)^{-1}d\varphi$$

for $i=1,2$ and $j=1,2$. In the above integrations, the values of the integrand $(\sin^2\varphi+e^{2\beta}\cos^2\varphi)^{-1}$ are distributed symmetrically, with a bell shape, around $\varphi=\pi/2(k_2=0)$, where they peak at 1. The width of the distribution that effectively contributes to the integral shrinks with time proportionally to e^{β}. We may note at this point that the integral $\int_0^{\pi}(\sin^2\varphi + e^{2\beta}\cos^2\varphi)^{-1}d\varphi=\pi e^{-\beta}$ for any β. At the same time, the variation of the values of the multiplying terms, $[(A_2^+/A)\delta_{i1} + (B_2^+/B)\delta_{i2}][(A_2^+/A)\delta_{j1}+(B_2^+/B)\delta_{j2}]^*\sin^2\varphi$ and $[(A_1^+/A)\delta_{i1} + (B_1^+/B)\delta_{i2}][(A_1^+/A)\delta_{j1}+(B_1^+/B)\delta_{j2}]^*$, with respect to β, is such that they show a nearly unchanged distribution inside the (shrinking) range of φ, which effectively determines the values of the integrals. Their distribution is also bell shaped, peaking at $\varphi=\pi/2$ $(k_2=0)$ where they reach fixed, finite values that depend only on η. Writing (5.6) as

$$R_{ij} \to \frac{q_0^2}{\pi}e^{2\beta\sqrt{1-\eta^2}}\int_0^{\pi} e^{f_{ij}(\varphi)}d\varphi, \tag{5.7}$$

the integrals now have the form necessary for applying the method of steepest descent[21] (also known as Laplace's method) with

$$f_{ij}^{\text{jet}}(\varphi) = \ln\left[\frac{[(A_1^+/A)\delta_{i1} + (B_1^+/B)\delta_{i2}][(A_1^+/A)\delta_{j1} + (B_1^+/B)\delta_{j2}]^*}{\sin^2\varphi + e^{2\beta}\cos^2\varphi}\right],$$
$$f_{ij}^{\text{vor}}(\varphi) = \ln\left[\frac{[(A_2^+/A)\delta_{i1} + (B_2^+/B)\delta_{i2}][(A_2^+/A)\delta_{j1} + (B_2^+/B)\delta_{j2}]^*\sin^2\varphi}{\sin^2\varphi + e^{2\beta}\cos^2\varphi}\right], \tag{5.8}$$

which are twice-differentiable, with their first derivative becoming zero at $\varphi=\pi/2$, where $f_{ij}(\varphi)$ maximize. Expanding $f_{ij}(\varphi)$ around $\varphi=\pi/2$ by Taylor's theorem,

$$f_{ij}(\varphi)=f_{ij}\left(\frac{\pi}{2}\right)+f'_{ij}\left(\frac{\pi}{2}\right)\left(\varphi-\frac{\pi}{2}\right)+\frac{1}{2}f''_{ij}\left(\frac{\pi}{2}\right)\left(\varphi-\frac{\pi}{2}\right)^2+O\left[\left(\varphi-\frac{\pi}{2}\right)^3\right], \tag{5.9}$$

we may approximate the asymptotic behavior of (5.6) and (5.7) as

$$R_{ij}\approx\frac{q_0^2}{\pi}e^{2\beta\sqrt{1-\eta^2}}e^{f_{ij}(\pi/2)}\int_0^{\pi}e^{(1/2)|f''_{ij}(\pi/2)|[\varphi-(\pi/2)]^2}d\varphi \tag{5.10}$$

(no implied summation over repeated indices), which reduces to

$$\frac{R_{ij}}{q_0^2}\approx\frac{1}{\pi}e^{2\beta\sqrt{1-\eta^2}}e^{f_{ij}(\pi/2)}\frac{2\sqrt{2}}{|f''_{ij}(\pi/2)|^{1/2}}\int_0^{\sqrt{2}\pi|f''_{ij}(\pi/2)|^{1/2}/4}e^{-u^2}du$$
$$=\frac{\sqrt{2}}{\sqrt{\pi}}e^{2\beta\sqrt{1-\eta^2}}\frac{e^{f_{ij}(\pi/2)}}{|f''_{ij}(\pi/2)|^{1/2}}\operatorname{erf}\left(\frac{\pi|f''_{ij}(\pi/2)|^{1/2}}{2\sqrt{2}}\right), \tag{5.11}$$

where $\operatorname{erf}(x)$ is the error function. Calculating the limits of $f_{ij}(\varphi)$ and $f''_{ij}(\varphi)$ at $\varphi\to\pi/2$, we derive analytical solutions of (5.11) for the approximate asymptotic behavior of the stresses, for $\eta^2\leq 1$. The value of $f_{ij}(\pi/2)$ depends only on η and remains fixed with time. On the other hand, the analytical limit of f''_{ij} as $\varphi\to\pi/2$ is proportional to $e^{2\beta}$, i.e.,

$$\lim_{\varphi\to\pi/2}f''_{ij}(\varphi)\sim e^{2\beta}, \tag{5.12}$$

which ensures $\operatorname{erf}[\sqrt{2}\pi|f''_{ij}(\pi/2)|^{1/2}/4]\to 1$ for large values of β and, as a result, the evolution of the Reynolds stress components R_{11}, R_{22}, and R_{33} approach for large times the following form:

$$\frac{R_{ij}^{\text{vor}}}{q_0^2}\to c_{ij}^{\text{vor}}(\eta)e^{\beta(2\sqrt{1-\eta^2}-1)},$$
$$\frac{R_{ij}^{\text{jet}}}{q_0^2}\to c_{ij}^{\text{jet}}(\eta)e^{\beta(2\sqrt{1-\eta^2}-1)},\quad i,j=1\text{ or }2. \tag{5.13}$$

The previous analysis is useful to capture the exact asymptotic behavior in terms of β, since the coefficients, $c_{ij}(\eta)$, are strict functions of η. This can also be understood from Fig. 2, where the numerical integrations of the full spectra relations (5.4) and (5.5), for the evolution of R_{11} and R_{22}, when multiplied by $e^{-\beta(2\sqrt{1-\eta^2}-1)}$, approach fixed constant values with

$$c_{11}^{\text{jet}}\sim\lim_{\varphi\to\pi/2}(A_1^+/A)^2=\frac{1}{4}\frac{(1-\sqrt{1-\eta^2})^2}{1-\eta^2},$$

$$c_{22}^{\text{jet}}\sim\lim_{\varphi\to\pi/2}(B_1^+/B)^2=\frac{1}{4}\frac{\eta^2}{1-\eta^2},$$

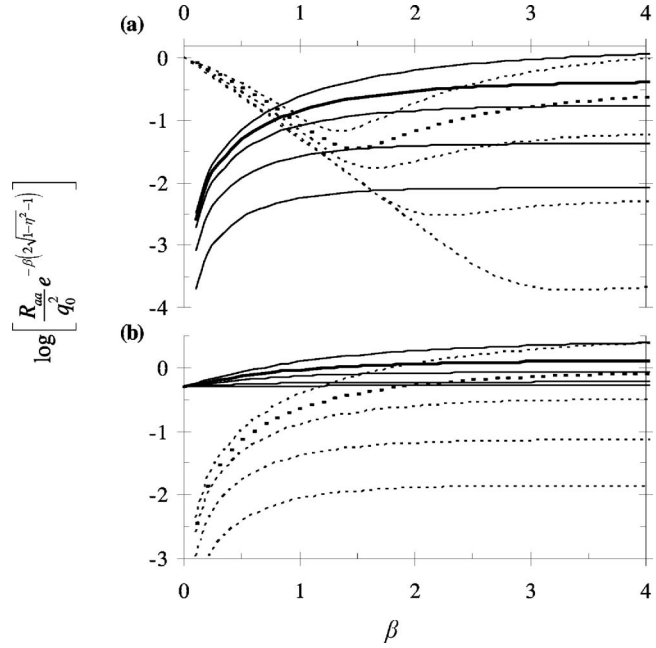

FIG. 2. Evolution of R_{11} (dashed) and R_{22} (solid), for the 2D solution with $k_1=0$ (a) when a jetal initialization and (b) when a vortical initialization is used, for $\eta=0.25$, 0.5, 0.75, 0.87 (bold), and 0.95. (upwards).

$$c_{12}^{\text{jet}}\sim\lim_{\varphi\to\pi/2}(A_1^+B_1^+/B^2)=\frac{1}{4}\frac{\eta(1-\sqrt{1-\eta^2})}{1-\eta^2},$$
$$c_{11}^{\text{vor}}\sim\lim_{\varphi\to\pi/2}(A_2^+/A)^2=\frac{1}{4}\frac{\eta^2}{1-\eta^2},$$
$$c_{22}^{\text{vor}}\sim\lim_{\varphi\to\pi/2}(B_2^+/B)^2=\frac{1}{4}\frac{(1+\sqrt{1-\eta^2})^2}{1-\eta^2},$$
$$c_{12}^{\text{jet}}\sim\lim_{\varphi\to\pi/2}(A_2^+B_2^+/B^2)=\frac{1}{4}\frac{\eta(1+\sqrt{1-\eta^2})}{1-\eta^2}. \tag{5.14}$$

As a result of (5.13), the stress components R_{11} and R_{22} increase exponentially when $\eta^2<3/4$, determining the unstable regime for the evolution of TKE. Note that for plane strain, the normal stresses do not depend *a priori* on the sign of the rotation of the frame. Recalling that the governing equation for TKE in the plane strain is

$$\partial q^2/\partial\beta=\partial(R_{11}+R_{22}+R_{33})/\partial\beta=-2R_{11}+2R_{22}, \tag{5.15}$$

and using the expressions (5.15), we calculate the respective asymptotic form for the remaining stress component R_{33},

$$R_{33}-c(\eta)+\frac{(3-2\sqrt{1-\eta^2})c_{22}(\eta)-(1+2\sqrt{1-\eta^2})c_{11}(\eta)}{(-1+2\sqrt{1-\eta^2})}\times e^{\beta(2\sqrt{1-\eta^2}-1)}, \tag{5.16}$$

where $c(\eta)$ is the constant of the integration. Thus, R_{33} also follows an exponential increase for values of $\eta^2<3/4$. The componentality of the 2D solution in this unstable regime remains 3C, with the normalized stress components, $r_{ij}=R_{ij}/q^2$, depending on the value of η^2, yet satisfying r_{11}

$<r_{22}<r_{33}$, as will be shown. The asymptotic states for the normalized values are the same for both the vortical and the jetal initialization.

It is instructive to look at the limiting states for specific values of the dimensionless frame rotation rate. For the most unstable case, without frame rotation, the limit of the spectral solutions (5.4) and (5.5) for $\eta^2 \to 0$ yields

$$E_{11}(\eta=0) = e^{-2\beta}E_{11}^0,$$
$$E_{22}(\eta=0) = \frac{e^2\beta(1+\cot^2\varphi)}{(e^2\beta\cot^2\varphi+1)^2}E_{22}^0, \tag{5.17}$$

which after the integration over the two wave numbers, and using (5.15), gives the stress components as

$$R_{11}/q_0^2 \sim e^{-2\beta}, \quad R_{22}/q_0^2 \sim e^{\beta}, \quad R_{33}/q_0^2 \sim e^{\beta}. \tag{5.18}$$

This result agrees well with the respective expression (2.8) by Townsend[5] for the 3D case (at least in terms of the more energetic R_{22} and R_{33} components). Note that the pressureless analysis (3.2) in this particular case results in a much stronger energy growth $\sim e^{2\beta}$.

For $\eta^2=3/4$, the stress components R_{11} and R_{22} reach constant values, and thus the R_{33} growth approaches a neutral, linear behavior,

$$R_{33}(\eta^2=3/4) \sim \beta. \tag{5.19}$$

As a result, the componentality of the turbulence tends to a 1C state with $r_{11}\to 0$, $r_{22}\to 0$, $r_{33}\to 1$, and, because d_{11} is identically 0, the turbulence approaches a 1D state with $d_{22}\to 1$, $d_{33}\to 0$. That is, it develops as sheets extending perpendicular to the x_2 axis with jetal velocity fluctuations along the axis of the frame rotation.

The same state is reached for values of $3/4<\eta^2\leq 1$, where the R_{11} and R_{22} diminish exponentially as $\sim e^{-\beta(1-2\sqrt{1-\eta^2})}$, and R_{33} approaches a constant value. As a result, the TKE does not increase. This is the initial, nonoscillatory part of the stable regime. For values of $\eta^2>1$, the exponent $\sqrt{1-\eta^2}$ becomes imaginary, and also the parameters $a_\pm$ are complex numbers, resulting in an oscillating behavior of the spectra, with a period proportional to $(\eta^2-1)^{-1/2}$. At the same time the term $(\sin^2\varphi+e^{2\beta}\cos^2\varphi)^{-1}$ in the expressions (5.4) and (5.5), when integrated over the entire range of φ, gives a stronger exponential decay $\sim e^{-\beta}$ stabilizing even faster the TKE.

VI. PRESSURE STRAIN-RATE CORRELATION

The rapid pressure strain-rate correlation tensor, which can be used for modeling applications, can be derived from the linear solution. It is defined as

$$T_{ij} = \frac{2}{\rho}\overline{ps_{ij}}, \tag{6.1}$$

where $s_{ij}=\frac{1}{2}(u_{i,j}+u_{j,i})$ is the fluctuating strain rate tensor. Equation (6.1) can be calculated by integrating the pressure-strain spectrum, $\Pi_{ij}=(-i/2\rho)\overline{\hat{p}(k_j\hat{u}_i+k_i\hat{u}_j)^*+(k_j\hat{u}_i+k_i\hat{u}_j)\hat{p}^*}$ over all wave numbers

$$T_{ij} = \int_{\mathbf{k}} \Pi_{ij}(\mathbf{k},\beta)d^3\mathbf{k}. \tag{6.2}$$

In our case of plane strain flow with $k_1=0$, Π_{ij} in cylindrical coordinates reduces to

$$\Pi_{11}=0, \quad \Pi_{22}=2\Gamma e^{2\beta}\frac{-2E_{22}+\eta E_{12}}{e^{2\beta}\cos^2\varphi+\sin^2\varphi}\cos^2\varphi,$$
$$\Pi_{33}=-\Pi_{22}, \quad \Pi_{12}=\Gamma e^{2\beta}\frac{-2E_{21}+\eta E_{11}}{e^{2\beta}\cos^2\varphi+\sin^2\varphi}\cos^2\varphi. \tag{6.3}$$

Due to the multiplication of the velocity spectra in (6.3) by the square of the wave-number component ($e^{2\beta}\cos^2\varphi$), these spectra vanish at the limit $\varphi=\pi/2$ (unlike the E_{11} and E_{22} forms). A profound maximum occurs in the vicinity of $\varphi=\pi/2$, but the location and the peak value depend on both β and η. In order to derive information regarding the statistics, we use the equations for the evolution of the stress components, which results in

$$\frac{T_{22}}{\Gamma}=\frac{dR_{22}}{d\beta}-2R_{22}+2\eta R_{12}, \quad \frac{T_{12}}{\Gamma}=\frac{dR_{12}}{d\beta}+\eta R_{11}-\eta R_{22}, \tag{6.4}$$

and making use of (5.13) we conclude that the pressure-strain correlations, inside the unstable regime, approach the following exponential behavior for large β:

$$\frac{T_{22}}{\Gamma}\to[c_{22}(2\sqrt{1-\eta^2}-3)+2\eta c_{12}]\exp^{\beta(2\sqrt{1-\eta^2}-1)},$$
$$\frac{T_{12}}{\Gamma}\to[c_{12}(2\sqrt{1-\eta^2}-1)-\eta c_{22}+\eta c_{11}]\exp^{\beta(2\sqrt{1-\eta^2}-1)}, \tag{6.5}$$

and the normalized values $\tau_{ij}=T_{ij}/(\Gamma R_{kk})$ reach asymptotically the values

$$\tau_{22}=r_{22}(2\sqrt{1-\eta^2}-3)+2\eta r_{12},$$
$$\tau_{12}=r_{12}(2\sqrt{1-\eta^2}-1)-\eta r_{22}+\eta r_{11}, \tag{6.6}$$

where r_{ij} are the respective asymptotic limits for the normalized stress components. For $\eta^2=3/4$, T_{ij} tend to constant values, and the normalized τ_{ij} approach zero, with a dependence $\sim\beta^{-1}$. In the stable regime, all the pressure strain-rate tensor components vanish relatively fast.

VII. COMPARISON OF THE 2D WITH THE 3D INITIALLY ISOTROPIC CASE

In Fig. 3, we present a comparison between the TKE evolution calculated by the analytical expressions derived here using the initially 2D-3C case with $k_1=0$, and the numerical solution of the 3D-3C initially isotropic initialization calculated using the Particle Representation Model (PRM) by Kassinos and Reynolds,[14] with a large enough number of particles to ensure the accuracy of the solution. The 2D analytical results are presented for a 2/3-1/3 weighted superposition (which corresponds to an initial equipartition of the energy as $r_{11}=r_{22}=r_{33}=1/3$) between the vortical and the

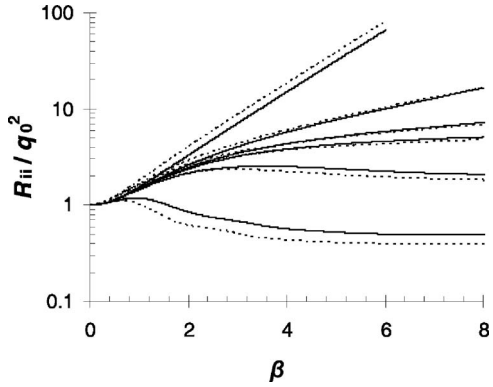

FIG. 3. Comparisons of the evolutions of the TKE, normalized with its initial value, for $\eta=0.5$, 0.8, $\sqrt{3}/2$, 0.9, 1, and 2 (clockwise), for the initially homogeneous 3D case calculated numerically with the PRM model (solid) and the 2D case with $k_1=0$ (dashed).

jetal initializations, respectively. From the comparison, it turns out that the 2D solution explains accurately the type of the TKE growth, while identifying the value of $-1+2\sqrt{1-\eta^2}$ as the correct parameter for the determination of the stability of the turbulent flow. Starting with the unstable cases, we notice the strong exponential evolution with time, which is of the form $\sim e^{(-1+2\sqrt{1-\eta^2})\beta}$. When η^2 reaches exactly the value 3/4, there is a departure from the exponential behavior toward a linear growth (neutral limit), while for $\eta^2>3/4$ the TKE stabilizes.

In Fig. 4, the evolutions of the normalized stresses r_{ij} and the structure dimensionality tensor components d_{ij} for the 2D approximation are illustrated for several η^2, and compared with the respective 3D-PRM exact numerical solutions. Despite the expected initial differences, as can be seen, for any value of η^2 the limiting states reached by the 2D case are in perfect agreement with the corresponding limiting states for initially 3D isotropic turbulence. The same agreement is also observed in the case of the normalized pressure-strain correlations in Fig. 5.

As mentioned, independently of the frame rotation rate, the d_{11} component in the 3D solution tends quickly to zero, which is why the 2D solution with $k_1=0$ proved to be a good approximation. For the unstable cases, the turbulence evolves fast toward a 2D-3C state, and the final distribution of the TKE among the different stress components, as well as the anisotropy of the dimensionality tensor in the 2D plane, depend on the value of η^2. The asymptotic states for the dimensionality and the componentality for the unstable cases are given in Table I. These values have been calculated using the numerical integration of the full spectral relations (5.4) and (5.5) at the limit when $\beta\to\infty$.

From Fig. 4, it becomes clear that for the neutral limit and for the stable cases, the turbulence evolves more slowly toward a fixed 1D-1C state with $r_{33}\to 1$, $d_{22}\to 1$. That is, the turbulence appears as sheets perpendicular to the x_2 axis with turbulent velocity fluctuations along the axis of the frame rotation.

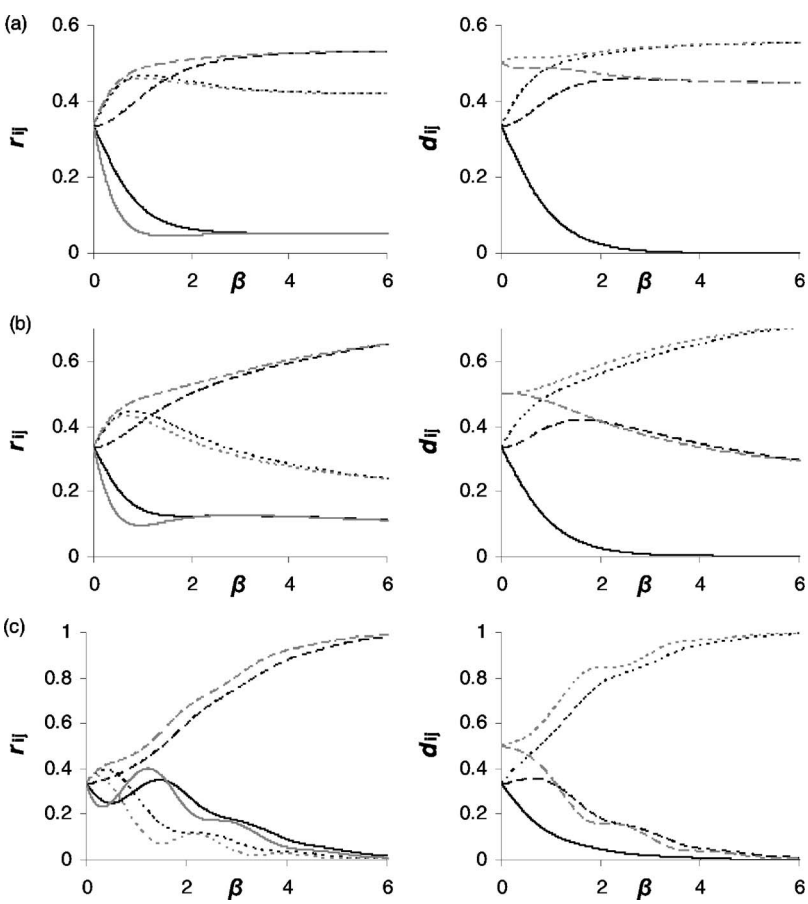

FIG. 4. Comparisons of the evolutions of the normalized stresses (left) and the structure dimensionality (right) components 11 (solid), 22 (short dashed), and 33 (long dashed) for $\eta=0.5$ (a), 0.8 (b), and 2 (c), for initially isotropic 3D turbulence (black) and 2D with $k_1=0$ (gray).

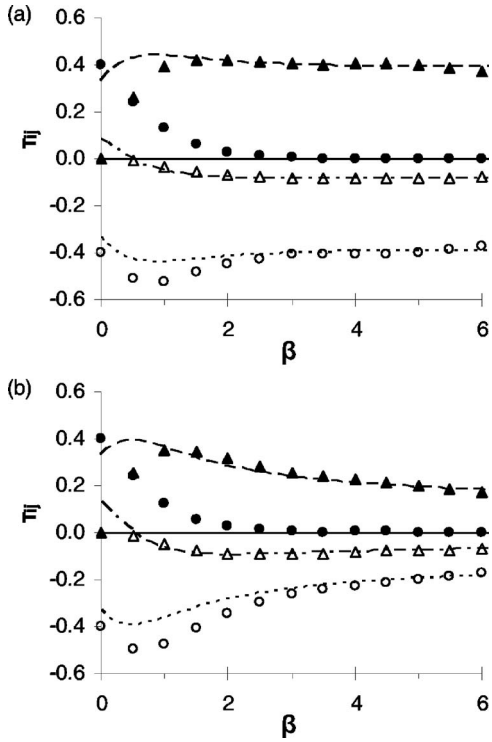

FIG. 5. Evolutions of the normalized pressure-strain correlation components 11 (continuous, solid circles), 22 (short dashed, open circles), 33 (long dashed, solid triangles), and 12 (dotted dashed, open triangles) for (a) $\eta=0.5$ and (b) $\eta=0.8$. Results from the PRM numerical solutions for initially isotropic 3D turbulence are shown as symbols and from the analytical solution for initially 2D-3C turbulence with $k_1=0$ as lines.

VIII. CONCLUSIONS

In the present study, we investigated turbulent plain strain flow in a rotating frame using RDT. Specifically, we determined the dependence of the evolution of the turbulent kinetic energy on the frame rotation rate. As shown, the oversimplified pressureless analysis cannot describe correctly the transition between the unstable and stable regimes, as well as the proper growth rate of the TKE. In contrast, the analytical 2D solution with $k_1=0$, which was derived here, maintains the crucial dependence on the pressure fluctuations, allowing for an accurate approximation of the 3D initially isotropic problem. The comparison with the 3D numerical results shows that despite expected initial differences, the 2D solution explains accurately the type of TKE growth, demonstrating that $-1+2\sqrt{1-\eta^2}$ (as found by the 2D analysis) is the proper parameter for the determination of the stability of the turbulent plain strain flow. Additionally, the calculated 2D asymptotic states of the turbulence, in terms of the normalized Reynolds stresses and the structure dimensionality tensor components, show a 2D-3C character for the unstable regime and a 1D-1C character elsewhere. This picture coincides with the exact three-dimensional numerical results. The findings of this work establish the framework for a generalized solution for hyperbolic flows in future work. Such generalized solutions will greatly improve our basic understanding of this important class of flows.

TABLE I. Asymptotic states of the normalized Reynolds stresses and structure dimensionality tensor components.

η	r_{11}	r_{22}	r_{33}	r_{12}	d_{22}	d_{33}
0	0	0.5	0.5	0	0.5	0.5
0.01	0.00002	0.49997	0.50001	0.00307	0.50002	0.49998
0.1	0.00205	0.49703	0.50092	0.03060	0.50176	0.49824
0.2	0.00819	0.48799	0.50382	0.06063	0.50719	0.49281
0.3	0.01845	0.47239	0.50916	0.08943	0.51683	0.48317
0.4	0.03278	0.44929	0.51793	0.11607	0.53179	0.46821
0.5	0.05089	0.41692	0.53219	0.13904	0.55422	0.44578
0.6	0.07173	0.37173	0.55654	0.15541	0.58857	0.41143
0.7	0.09115	0.30529	0.60356	0.15810	0.646	0.354
0.75	0.09579	0.25723	0.64698	0.14834	0.69279	0.30721
0.79	0.09153	0.20464	0.70383	0.12897	0.74872	0.25128
0.8	0.08829	0.18829	0.72342	0.12140	0.76701	0.23299
0.85	0.04045	0.06724	0.89231	0.04887	0.91309	0.08691
0.86	0.01788	0.02818	0.95394	0.02101	0.96321	0.03679
0.865	0.00332	0.0051	0.99158	0.00385	0.99331	0.00669
0.866	0.00008	0.00013	0.99979	0.00010	0.99983	0.00017
$\sqrt{3}/2$	0	0	1	0	1	0

ACKNOWLEDGMENTS

The authors would like to thank an anonymous referee who provided valuable suggestions that stimulated some of the analysis contained in this work. This work has been performed under the UCY-CompSci project, a Marie Curie Transfer of Knowledge (TOK- DEV) grant (Contract No. MTKD-CT-2004-014199) funded by the CEC under the 6th Framework Program, and under the WALLTURB project (a European synergy for the assessment of wall turbulence, Contract No. AST4-CT-2005-516008), both funded by the CEC under the 6th framework program.

[1] J. Bardina, J. H. Ferziger, and W. C. Reynolds, "Improved turbulence models based on large-eddy simulation of homogeneous incompressible turbulent flows," Technical Report No. TF-19, Mechanical Engineering Department, Stanford University, Stanford, CA (1983).
[2] G. Brethouwer, "The effect of rotation on rapidly sheared homogeneous turbulence and passive scalar transport. Linear theory and direct numerical simulation," J. Fluid Mech. **542**, 305 (2005).
[3] S. B. Pope, *Turbulent Flows* (Cambridge University Press, Cambridge, UK, 2000), p. 421.
[4] H. Hanazaki and J. C. R. Hunt, "The structure of unsteady stably stratified turbulence with mean shear," J. Fluid Mech. **507**, 1 (2004).
[5] A. A. Townsend, *The Structure of Turbulent Shear Flow*, 2nd ed. (Cambridge University Press, Cambridge, UK, 1976).
[6] A. M. Savill, "Recent developments in rapid distortion theory," Annu. Rev. Fluid Mech. **19**, 531 (1987).
[7] J. C. R. Hunt and D. J. Carruthers, "Rapid distortion theory and the 'problems' of turbulence," J. Fluid Mech. **212**, 497 (1990).
[8] A. Salhi, C. Cambon, and C. G. Speziale, "Linear stability analysis of plane quadratic flows in a rotating frame with applications to modeling," Phys. Fluids **9**, 2300 (1997).
[9] P. Bradshaw, "The analogy between streamline curvature and buoyancy in turbulent shear flow," J. Fluid Mech. **36**, 177 (1969).
[10] C. G. Speziale and N. Mac Giolla Mhuiris, "Scaling laws for homogeneous turbulent shear flows in a rotating frame," Phys. Fluids A **1**, 294 (1989).
[11] S. C. Kassinos, W. C. Reynolds, and M. M. Rogers, "One-point turbulence structure tensors," J. Fluid Mech. **428**, 213 (2001).
[12] S. C. Kassinos, C. A. Langer, G. Kalitzin, and G. Iaccarino, "A simplified structure-based model using standard turbulence scale equations: Compu-

tation of rotating wall-bounded flows," Int. J. Heat Fluid Flow **27**, 653 (2006).
[13]E. Akylas, S. C. Kassinos, and C. A. Langer, "Rapid shear of initially anisotropic turbulence in a rotating frame," Phys. Fluids **19**, 025102 (2007).
[14]S. C. Kassinos and W. C. Reynolds, "Structure-based modeling for homogeneous MHD turbulence," *Annual Research Briefs* (Stanford University and NASA Ames Research Center: Center for Turbulence Research, Stanford, CA, 1999), pp. 301–315.
[15]R. S. Rogallo, "Numerical experiments in homogeneous turbulence," NASA Tech. Memo. 81315 (1981).
[16]R. R. Lagnado, N. Phan-Thien, and L. G. Leal, "The stability of two-dimensional linear flows," Phys. Fluids **27**, 1094 (1984).
[17]M. J. Lee, U. Piomelli, and W. C. Reynolds, "Useful formulas in the rapid distortion theory of homogeneous turbulence," Phys. Fluids **29**, 3471 (1986).
[18]F. S. Godeferd, "Distorted turbulence submitted to frame rotation: DNS and LES results," *Annual Research Briefs* (Stanford University and NASA Ames Research Center: Center for Turbulence Research, Stanford, CA, 1995), pp. 175–193.
[19]C. G. Speziale, "Some interesting properties of two-dimensional turbulence," Phys. Fluids **24**, 1425 (1981).
[20]C. Cambon, N. N. Mansour, and F. S. Godeferd, "Energy transfer in rotating turbulence," J. Fluid Mech. **337**, 303 (1997).
[21]A. Erdelyi, *Asymptotic Expansions* (Dover, New York, 1956).